Gβγ Interferes with Ca^{2+}-Dependent Binding of Synaptotagmin to the Soluble N-Ethylmaleimide-Sensitive Factor Attachment Protein Receptor (SNARE) Complex[S]

Eun-Ja Yoon, Tatyana Gerachshenko, Bryan D. Spiegelberg, Simon Alford, and
Heidi E. Hamm

Department of Pharmacology, Vanderbilt University Medical School, Nashville, Tennessee (E.J.Y., B.D.S., H.E.H.); and
Department of Biological Sciences, University of Illinois at Chicago, Chicago, Illinois (T.G., S.A.).

ABSTRACT

Presynaptic inhibitory G protein-coupled receptors (GPCRs) can decrease neurotransmission by inducing interaction of Gβγ with the soluble N-ethylmaleimide-sensitive factor attachment protein receptor (SNARE) complex. We have shown that this action of Gβγ requires the carboxyl terminus of the 25-kDa synaptosome-associated protein (SNAP25) and is downstream of the well known inhibition of Ca^{2+} entry through voltage-gated calcium channels. We propose a mechanism in which Gβγ and synaptotagmin compete for binding to the SNARE complex. Here, we characterized the Gβγ interaction sites on syntaxin1A and SNAP25 and demonstrated an overlap of the Gβγ- and synaptotagmin I -binding regions on each member of the SNARE complex. Synaptotagmin competes in a Ca^{2+}-sensitive manner with binding of Gβγ to SNAP25, syntaxin1A, and the assembled SNARE complex. We predict, based on these findings, that at high intracellular Ca^{2+} concentrations, Ca^{2+}-synaptotagmin I can displace Gβγ binding and the Gβγ-dependent inhibition of exocytosis can be blocked. We tested this hypothesis in giant synapses of the lamprey spinal cord, where 5-HT works via Gβγ to inhibit neurotransmission (Blackmer et al., 2001). We showed that increased presynaptic Ca^{2+} suppresses the 5-HT- and Gβγ-dependent inhibition of exocytosis. We suggest that this effect may be due to Ca^{2+}-dependent competition between Gβγ and synaptotagmin I for SNARE binding. This type of dynamic regulation may represent a novel mechanism for modifying transmitter release in a graded manner based on the history of action potentials that increase intracellular Ca^{2+} concentrations and of inhibitory signals through G$_i$-coupled GPCRs.

Modification of neurotransmitter release by presynaptic G protein-coupled receptors (GPCRs) is ubiquitous and vital to nervous system function. Gβγ inhibits synchronous exocytosis directly at the SNARE complex, the heart of the fusion machinery (Silinsky, 1984; Man-Son-Hing et al., 1989; Blackmer et al., 2001, 2005; Takahashi et al., 2001; Chen et al., 2005; Gerachshenko et al., 2005) and consequently modifies the quantal size of release by causing transient fusion of vesicles in both lamprey giant synapses and mammalian chromaffin cells (Chen et al., 2005; Photowala et al., 2006). G

proteins may also inhibit exocytosis through inhibition of voltage-gated calcium channels, blunting the influx of Ca^{2+} required for exocytosis (Herlitze et al., 1996; Ikeda, 1996).

Synaptotagmin I is believed to mediate the requirement for Ca^{2+} in the initiation of exocytosis. Before the fusion event, vesicles are primed by formation of a stable protein structure, the ternary SNARE complex, comprising the plasma membrane t-SNAREs SNAP25 and syntaxin and the vesicular SNARE VAMP2 (Fig. 1A). Synaptotagmin, as the putative Ca^{2+} sensor, is thought to act as the trigger by which Ca^{2+} influx effects the fusion of primed vesicles (Bai et al., 2004; Maximov and Sudhof, 2005; Wang et al., 2006).

Given its central role in triggering exocytosis, interactions between synaptotagmins and the SNARE complex have been studied extensively. Upon Ca^{2+} binding to its C2 domains (Fig. 1A) during regulated exocytosis, synaptotagmin interacts with phospholipids and the SNARE complex (Perin et

ABBREVIATIONS: GPCR, G protein-coupled receptor; SNARE, soluble N-ethylmaleimide-sensitive factor attachment protein receptor; t-SNARE, target membrane-associated snare; SNAP25, 25-kDa synaptosome-associated protein; DTT, dithiothreitol; OG, n-octyl β-D-glucopyranoside; PAGE, polyacrylamide gel electrophoresis; GST, glutathione transferase; MIANS, 2-(4′-maleimidylanilino) naphthalene-6-sulfonic acid; MOPS, 3-(N-morpholino)propanesulfonic acid; BoNT/A, botulinum toxin A; EPSC, excitatory postsynaptic current; 5-HT, 5-hydroxytryptamine.

al., 1990; Schiavo et al., 1997). This interaction occurs through the H3 SNARE domain of syntaxin1A and the C terminus of SNAP25 (Bennett et al., 1992; Chapman et al., 1995; Gerona et al., 2000; Bai et al., 2004). Although the mechanism by which the SNARE complex initiates fusion is under debate (Rizo et al., 2006), interactions with synaptotagmin may cause stabilized ternary SNAREs to zip up, uniting the vesicular and plasma membranes (Margittai et al., 1999; Sorensen et al., 2006). Other evidence suggests that ternary SNARE complex formation is a concerted process with more than one transition state during initial and sustained dilation of a protein fusion pore (Han and Jackson, 2006).

Despite the controversy regarding SNARE complex-mediated membrane fusion, widespread consensus holds that synaptotagmin is the Ca^{2+} sensor for stimulated exocytosis and may provide the cue for full fusion versus kiss-and-run fusion. Mutagenesis studies, for example, indicate that fusion is inhibited in the presence of synaptotagmin mutants with diminished SNARE interactions (Bai et al., 2004). Furthermore, overexpression of different isoforms of synaptotagmin in PC-12 cells leads to different fusion pore opening durations, suggesting that the interaction of synaptotagmin with the SNARE complex and the membrane affects the nature of fusion pore formation and dilation (Wang et al., 2001). Gβγ signaling is another mediator of fusion pore dynamics (Blackmer et al., 2005; Chen et al., 2005; Gerachshenko et al., 2005; Photowala et al., 2006), but it is unclear how the Ca^{2+}-dependent synaptotagmin/SNARE complex interaction is actively modulated by Gβγ (Searl and Silinsky, 2005).

We have shown that the nine C-terminal residues of SNAP25 that interact with synaptotagmin provide an important binding site for Gβγ. The resulting Gβγ/SNARE interaction inhibits transmitter release in vertebrate central synapses and mammalian neuroendocrine cells (Blackmer et al., 2005; Gerachshenko et al., 2005). We now identify Gβγ binding sites on the SNARE complex. In addition, we identify a role for Ca^{2+} and demonstrate competition between Gβγ and synaptotagmin for binding to SNARE complexes. We propose that modulation of exocytosis is subject to convergent and complementary pathways directed to alteration of synaptotagmin/SNARE complex interactions in which presynaptic Ca^{2+} both stimulates fusion and modifies the impact of $G_{i/o}$-coupled inhibitory GPCRs on exocytosis.

Materials and Methods

Plasmids. The open reading frames for the SNARE component proteins were subcloned into the pGEX6p1 vector (GE Healthcare, Chalfont St. Giles, Buckinghamshire, UK) for expression in bacteria. Individual truncation mutants were generated via a PCR-based strategy.

SNARE Protein Purification. Recombinant bacterially expressed glutathione transferase (GST) fusion proteins were expressed in *Escherichia coli* strain BL21(DE3). Protein expression was induced with 0.1 mM isopropyl β-D-thiogalactoside for 16 h at room temperature. Bacterial cultures were pelleted, washed with $1\times$ phosphate-buffered saline, and then resuspend in lysis buffer [50 mM NaCl, 50 mM Tris, pH 8.0, 5 mM EDTA, 0.1% Triton X-100, 2 mM phenylmethylsulfonyl fluoride, and 1 mM dithiothreitol (DTT)]. Cells were lysed with a sonic dismembrator at 4°C. GST-SNAP25
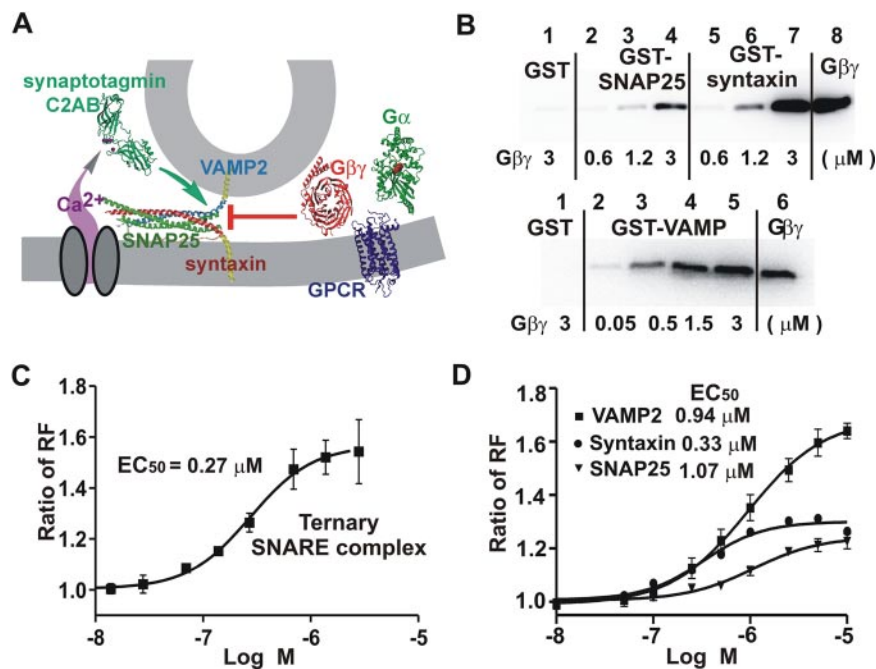

Fig. 1. Gβγ binds individual SNARE proteins and their ternary complex. A, the SNAREs in the primed state and their relationship to synaptotagmin. We hypothesize that Gβγ counteracts synaptotagmin by interacting with the C-terminal region of the SNARE complex. B, Gβγ interacts with SNAP25 and syntaxin1A in a GST pulldown assay (top). Equimolar amounts of GST (lane 1), GST-SNAP25 (lanes 2–4), or GST-syntaxin1A (lanes 5–7) were incubated with the noted concentrations of $G_{\beta_1}\gamma_2$. Precipitated Gβ was detected with an anti-pan Gβ antibody. Purified Gβγ was included as a loading control (lane 8). Gβγ interacts directly with VAMP2 (bottom). GST (lane 1), GST-VAMP2 (lanes 2–5), and a Gβγ loading control (lane 6). C, quantification of the interaction of Gβγ with the ternary SNARE complex with fluorescent binding. Purified Gβγ was labeled with MIANS environmentally sensitive fluorescence probe. The fluorescence change was monitored by spectrofluorometry using 20 nM labeled Gβγ and various concentrations of SNARE complex. Fluorescence change was normalized by basal level of labeled Gβγ fluorescence and represented as relative fluorescence. Increasing concentrations of the SNARE complex induced enhanced fluorescence of MIANS-$G_{\beta_1}\gamma_1$, indicating formation of a Gβγ/SNARE interaction. The data presented ratio of relative fluorescence (RF) at each different protein concentration ($n = 3$). D, affinities of individual SNARE components for Gβγ. Using the fluorescent binding assay, strengths of binding to 20 nM MIANS-Gβγ were found to follow the order syntaxin1A ($EC_{50} = 0.33$ μM), VAMP2 (0.94 μM), and SNAP25 (1.07 μM).

and GST-VAMP2 were purified from cleared lysates by affinity chromatography on glutathione-agarose (GE Healthcare), following the manufacturer's instructions. While the proteins were bound to the column, the buffer was exchanged to 20 mM HEPES, pH 7.4, 100 mM NaCl, 0.05% n-octyl β-D-glucopyranoside (OG), and 5 mM dithiothreitol. In some cases, the proteins were eluted by cleaving from GST with PreScission protease (GE Healthcare) for 4 h at 4°C and then dialyzed extensively against 20 mM HEPES, pH 7.0, 80 mM KCl, 20 mM NaCl, and 0.05% OG. GST-syntaxin1A (lacking the transmembrane domain) was purified from the sonicated bacterial supernatant by affinity chromatography on glutathione-agarose (GE Healthcare) in 10 mM HEPES, pH 7.4, 0.05% OG, and 2 mM DTT. Protein concentrations were determined with a Bradford assay kit (Pierce, Rockford, IL), and purity was verified by SDS/PAGE analysis.

Binary and Ternary SNARE Complex Reassembly. An equimolar ratio (3 μM) of GST-syntaxin1A on glutathione-agarose and SNAP25 were incubated overnight at 4°C in 20 mM HEPES, pH 7.4, 100 mM NaCl, 0.1% OG, and 2.0 mM dithiothreitol. The binary t-SNARE complex was washed three times with phosphate-buffered saline and eluted from the column by removing GST with PreScission protease (GE Healthcare) for 4 h at 4°C. Equimolar protein-protein interaction was confirmed by SDS-PAGE/Coomassie staining analysis. To reassemble ternary SNARE complex, an equimolar ratio (3 μM) of GST-syntaxin1A on glutathione-agarose, VAMP2, and SNAP25 was incubated overnight at 4°C in 20 mM HEPES, pH 7.4, 100 mM NaCl, 0.1% OG, and 2.0 mM DTT. The SNARE proteins were washed and eluted from the column by removing GST. SDS- and heat-stable SNARE complex formation was verified by SDS/PAGE analysis with or without a 15-min incubation at 100°C.

Gβγ Purification and Labeling. $G\beta_1\gamma_1$ was purified from bovine retina as described previously (Mazzoni et al., 1991). Recombinant $G\beta_1\gamma_2$ was expressed in Sf9 cells and purified via a His$_6$ tag on $G\gamma_2$ using nickel-nitrilotriacetic acid affinity chromatography (Sigma-Aldrich, St. Louis, MO). Fluorescence labeling of $G\beta_1\gamma_1$ and binding assays were conducted as described previously (Phillips and Cerione, 1991). In brief, purified $G\beta_1\gamma_1$ was dialyzed into labeling buffer (20 mM HEPES, pH 7.4, 5 mM MgCl$_2$, 150 mM NaCl, and 10% glycerol), then mixed with 2-(4′-maleimidylanilino)naphthalene-6-sulfonic acid (MIANS) in a 5-fold molar excess. The reaction proceeded for 3 h at 4°C before quenching with 5 mM 2-mercaptoethanol. The MIANS-$G\beta_1\gamma_1$ complex was separated from unreacted MIANS using a PD-10 desalting column (GE Healthcare). MIANS-$G\beta_1\gamma_1$ was stored in aliquots at −80°C.

Fluorescence Binding and Competition Assay. All fluorescence measurements were performed in a fluorescence spectrophotometer (Cary Eclipse; Varian, Inc., Palo Alto, CA) at room temperature. In general, MIANS-$G\beta_1\gamma_1$was diluted into 0.5 ml of assay buffer (20 mM HEPES, pH 7.5, 5 mM MgCl$_2$, 1 mM DTT, 0.1 M NaCl, and 1 mM EDTA) to a final concentration of 20 nM. The MIANS fluorescence was monitored with excitation at 322 nm and emission at 417 nm. All proteins purified as GST fusion proteins were cleaved from GST with PreScission protease (GE Healthcare) before analysis. The fluorescent changes caused by the addition of SNARE complexes were monitored continuously. Note that the amplitude of the fluorescence increase is not a measure of the affinity of the complex; rather, it reflects the specific site on fluorescently labeled Gβγ of interaction with each protein. There was no nonspecific binding of the free probe to the SNARE proteins and MIANS-Gβγ was resistant to photobleaching under experimental conditions (data not shown). For Gβγ/synaptotagmin competition assays, various concentrations of synaptotagmin with SNARE proteins were added to labeled $G\beta_1\gamma_1$ with the noted Ca^{2+}concentrations, and fluorescence changes were monitored. The EC$_{50}$ concentrations were determined by sigmoidal curve fitting using Prism software (GraphPad Software, San Diego, CA).

GST Pull-Down Assay. GST-SNAP25, GST-VAMP2, and GST-syntaxin1A (5 μg of each protein) were incubated with various amount of $G\beta_1\gamma_2$ proteins for 1 h at 4°C and washed three times with

assay buffer (20 mM HEPES, pH 7.0, 80 mM KCl, 20 mM NaCl, and 0.1% OG). The complex was eluted with 20 μl of SDS sample buffer followed by separation via SDS-PAGE. Precipitated Gβ was detected using Western blotting with a rabbit anti-pan Gβ antibody (Santa Cruz Biotechnology, Santa Cruz, CA).

Electrophysiology and Microinjection. Lamprey spinal cord preparations (*Petromyzon marinus*) were performed as described previously (Wickelgren, 1977). Whole-cell patch-clamp recordings were achieved with a modified blind technique (Blanton et al., 1989) using pipettes (5–10 MΩ) containing solution of the following composition: 102.5 mM MeSO$_4$, 1 mM NaCl, 1 mM MgCl$_2$, 5 mM HEPES, and 0.05 mM EGTA, brought to a pH of 7.4 with KOH. All paired recordings to measure the effect of protein injection in this study were made at a minimum of 5 min after injection and less than 100 μm from the presynaptic injection site. Recombinant $G\beta_1\gamma_2$ protein was stored at −20°C in a solution containing 100 mM MeSO$_4$, 5 mM HEPES, and 0.05 mM EGTA at pH of 7.4. Concentrations ranged from 3 to 5 mg/ml. For microinjection into the presynaptic terminal, 50% (by volume) of 1 M KMeSO$_4$ was added to the $G\beta_1\gamma_2$-containing solution. Protein was pressure microinjected through presynaptic microelectrodes using Picospritzer II (General Valve, Fairfield, NJ).

Imaging. Fluorescence images were recorded with a modified confocal microscope (MRC600; Bio-Rad Laboratories, Hercules, CA) run with custom software available at http://alford.bios.uic.edu. Reticulospinal axons were labeled retrogradely with a dextran amine-conjugate form of the Ca^{2+}-sensitive dye Fluo-4 (high affinity; Invitrogen, Carlsbad, CA). The dye was applied using a suction pipette fitted to the cut end, immediately after the end of the spinal cord was cut. The tissue was then incubated overnight for the dye to be transported throughout the axons. Images were collected at high speed by scanning a laser over a single line at 500 Hz. Imaging data were analyzed using NIH ImageJ software (http://rsb.info.nih.gov/ij/) on a Macintosh computer. ImageJ was used to calculate the brightness value (range of possible values, 10 bit) for each pixel in a field of view. For each individual axon of interest, the brightness values were measured, and after background subtraction, images were normalized to the baseline level of fluorescence to give $(F + 1)/F$ values.

Calibration of the Ca^{2+} Sensitive Dyes. The dye sensitivity to Ca^{2+} was determined using the same optical path (confocal microscope) that was used to measure Ca^{2+} transients in the tissue. Dyes (5 μM) were prepared in blends of two Ca^{2+} buffer standards (10 mM K$_2$EGTA, 100 mM KCl, and 30 mM MOPS) and (10 mM CaEGTA, 100 mM KCl, and 30 mM MOPS) both at pH 7.2 (Invitrogen) to make an 11-point standard curve. The absolute Ca^{2+} values of the mix were corrected for the low temperatures used in this study (10°C). The dye buffer mix was placed between cover slips cooled from below with a liquid cooling system to 10°C and imaged from above with the 40× water immersion lens.

Western blots are representative of at least three independent experiments. Data points are presented as mean ± S.E.M. (∗, $p < 0.01$; ∗∗, $p < 0.001$, two-tailed Student's t test).

Results

Gβγ Interacted with Individual SNARE Proteins and Ternary SNARE Complex. To understand the relationship between Gβγ and the SNARE complex in the modulation of exocytosis, we characterized sites of interaction by two complementary in vitro approaches, GST pulldown assays and fluorescent binding assays. In GST pulldowns, both components of the t-SNARE (syntaxin1A and SNAP25) interacted with Gβγ individually. In addition, the vesicular SNARE component, VAMP2, was found to interact directly with Gβγ (Fig. 1B). To demonstrate that the GST pulldown assay provides specific binding, we performed pulldown assays with Gα subunit and heterotrimeric G protein that contains Gαβγ. The Gβγ subunit, but not the Gα subunit or the heterotri-

meric G proteins, interacts with SNARE proteins, suggesting that G protein interaction with SNARE occurs upon inhibitory G protein-coupled receptor activation that induces Gα and Gβγ dissociation (Supplementary Figure S1).

To quantify the relative contributions to Gβγ binding by the individual SNARE components, we employed a sensitive and quantitative fluorescence assay for measuring protein-protein interactions (Phillips and Cerione, 1991). $G\beta_1\gamma_1$ was labeled with the environmentally sensitive fluorescent probe MIANS. This probe serves to report interaction with a binding partner because it undergoes enhanced fluorescence when the local environment becomes more hydrophobic. In these assays, labeled Gβγ (final concentration, 20 nM) was used, whereas interactions with different concentrations of individual SNARE proteins or complexes were assessed through fluorescence intensity changes. Therefore, apparent affinities were estimated by determining concentrations of binding proteins at which MIANS fluorescence reached 50% of maximum (EC_{50}).

This assay was used to quantify the interaction of Gβγ with the ternary SNARE complex and its constituent proteins (Fig. 1, C and D). The ternary SNARE complex indeed caused a dose-dependent increase in the fluorescence of MIANS-Gβγ, consistent with our previous findings that Gβγ and the SNARE complex interact in vitro (Blackmer et al., 2001, 2005) (Fig. 1C and $EC_{50} = 0.27$ μM). Likewise, we tested the apparent Gβγ-binding affinities of the individual SNARE components (Fig. 1D). Each of the three components caused a fluorescence increase, confirming direct interactions. The relative affinities followed the order syntaxin1A ($EC_{50} = 0.33$ μM), VAMP2 (0.94 μM), and SNAP25 (1.07 μM).

Gβγ Interacted with the Syntaxin1a H3 Motif and the C Terminus of SNAP25. Syntaxin1A has two major regions, the H3 SNARE domain and the modulatory Habc region (Fig. 2A). Truncation mutants representing the two

major syntaxin1A regions were generated (Fig. 2A), and EC_{50} values for binding to 20 nM MIANS-labeled Gβγ were determined. The syntaxin1A H3 domain showed a right-shifted binding curve ($EC_{50} = 0.89$ μM; Fig. 2B) relative to the entire molecule ($EC_{50} = 0.33$ μM). Syntaxin1A (1–190) did not induce a significant Gβγ fluorescence change. These results, which were confirmed by GST pulldown assays (data not shown), indicate that Gβγ binds to the syntaxin1A H3 SNARE domain. However, because Gβγ bound to the H3 domain with an affinity lower than that for intact syntaxin1A, we cannot rule out a masked minor contribution of the Habc domain or the possibility that the isolated domain does not fold optimally (Jarvis et al., 2002).

Recent evidence suggests that nine amino acids from the C terminus of SNAP25 are crucial for interaction with Gβγ as well (Blackmer et al., 2005; Gerachshenko et al., 2005). Botulinum toxin A (BoNT/A) treatment, which removes nine C-terminal residues of SNAP25 (SNAP25Δ9) (Fig. 2C), diminishes Gβγ-mediated inhibition of exocytosis (Blackmer et al., 2005; Gerachshenko et al., 2005). In addition, a ternary SNARE complex comprising VAMP2, syntaxin1A, and SNAP25Δ9 shows reduced Gβγ binding compared with the wild-type SNARE complex (Gerachshenko et al., 2005). Here, we quantified the direct interaction of Gβγ with the C terminus of SNAP25. A truncation mutant of SNAP25 that mimics the BoNT/A cleavage product (SNAP25Δ9) was analyzed for its binding to Gβγ. Relative to full-length SNAP25, SNAP25Δ9 showed significantly decreased affinity for Gβγ (Fig. 2D).

In presynaptic terminals of neurons in situ and in cultured PC-12 and chromaffin cells, BoNT/E, which cleaves 26 amino acids from the C terminus of SNAP25 (Fig. 2C), inhibits Ca^{2+}-dependent exocytosis (Ferrer-Montiel et al., 1998; Chen et al., 2001), consistent with an observed loss of interaction between synaptotagmin and SNAP25 (Chen et al., 1999; Gerona et al., 2000). We investigated whether a further trun-
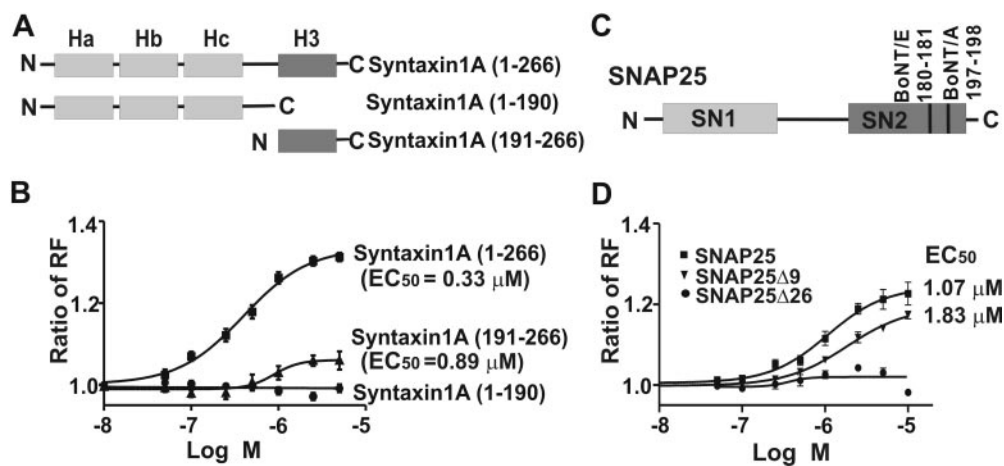

Fig. 2. Gβγ interacts with the H3 domain of syntaxin1A and C terminus of SNAP25. A, domain organization of syntaxin1A. Fluorescent binding assays were performed with three variants of syntaxin1A: 1–266, which contains the Habc and H3 domains but lacks a transmembrane region; 1–190, which contains the Habc domain and the Habc-H3 linker region; and 191–266, which contains the H3 domain. B, quantification of the Gβγ/syntaxin1A interaction. Syntaxin1A variants were cleaved from GST, and interaction with MIANS-Gβγ was detected by increased fluorescence output. The data represented the ratio of RF at each different protein concentration. MIANS-Gβγ (20 nM) was found to interact with syntaxin1A (1–266) with an EC_{50} of 0.33 μM and with the H3 domain syntaxin1A (191–266) with an EC_{50} of 0.89 μM, whereas no significant interaction with syntaxin1A (1–190) was observed. C, domain organization of SNAP25. SNAP25 contains two SNARE motifs (SN1 and SN2). The C terminus is cleaved specifically by two botulinum toxins, BoNT/E (between amino acids 180 and 181) and BoNT/A (196 and 197). D, removal of the C terminus of SNAP25 reduces affinity for Gβγ. SNAP25 truncation mutants mimicking cleavage by BoNT/A (SNAP25Δ9) or BoNT/E (SNAP25Δ26) were tested for affinity for Gβγ using the fluorescent binding assay. MIANS-Gβγ (20 nM) was found to interact with SNAP25 with an EC_{50} of 1.07 μM and with SNAP25Δ9 (mimics BoNT/A cleavage) with an EC_{50} of 1.83 μM, whereas no significant interaction with SNAP25Δ26 (mimics BoNT/E cleavage).

1214 Yoon et al.

cated SNAP25 (SNAP25Δ26) also weakens binding to Gβγ. Fluorescent binding assays demonstrated that deletion of 26 amino acids caused a great loss of Gβγ binding (Fig. 2D). These data indicate that 26 C-terminal amino acids of SNAP25 are also critical for Gβγ binding.

Gβγ and Synaptotagmin Competed in Binary and Ternary SNARE Complexes in a Ca^{2+}-Dependent Manner. It is noteworthy that the Gβγ-binding domains of the SNARE complex, the syntaxin1A H3 domain and the C terminus of SNAP25, are also known to constitute functionally important Ca^{2+}-dependent synaptotagmin binding sites (Chapman et al., 1995; Gerona et al., 2000). The overlapping of binding sites suggests that there might be competition between Gβγ and synaptotagmin on the complexed SNAREs. To test whether Gβγ competes with synaptotagmin for binding to SNARE proteins in complex, we conducted competition assays in vitro. We used a mutant of synaptotagmin I (K326A, K327A) that exhibits wild-type SNARE binding affinity but holds a reduced propensity to oligomerize and to form insoluble aggregates in response to high concentrations of Ca^{2+} (Bai et al., 2004). In fluorescent binding assays, synaptotagmin does not interact significantly with MIANS-Gβγ (data not shown). We therefore tested competition between Gβγ and synaptotagmin for binding to the binary t-SNARE complex, comprising syntaxin1A and SNAP25. The interaction between Gβγ and binary t-SNARE complex in the

absence of synaptotagmin was normalized to 100%. In 50 μM Ca^{2+}, the interaction between MIANS-Gβγ and 1 μM binary t-SNARE complex was almost completely inhibited by 250 nM synaptotagmin I (Fig. 3A). Increasing synaptotagmin concentrations competed more effectively with Gβγ, resulting in reduced fluorescence changes (Fig. 3B), further indicating that Gβγ and synaptotagmin compete for SNARE binding.

Synchronous vesicle fusion is initiated by Ca^{2+}, but additional Ca^{2+} influx may modify large dense core vesicle fusion properties and possibly alter the quantal size of synaptic neurotransmitter release (Elhamdani et al., 2001, 2006; Harata et al., 2006). Because this modulation may reflect the Ca^{2+} sensitivity of synaptotagmin (Morimoto et al., 1995), we tested whether competition with Gβγ is also Ca^{2+} sensitive. We found that the competition between synaptotagmin and Gβγ for binary t-SNARE complex binding is dependent on intracellular Ca^{2+} concentrations. In buffer lacking Ca^{2+}, synaptotagmin caused a slight but statistically significant inhibition of the ability of t-SNAREs to increase the fluorescence of MIANS-Gβγ (Fig. 3C), possibly because of a limited Ca^{2+}-independent interaction between synaptotagmin and t-SNAREs (Bennett et al., 1992; Sollner et al., 1993). However, upon addition of physiologically relevant concentrations of Ca^{2+}, we observed an increased inhibition of Gβγ binding by synaptotagmin, with maximum effectiveness at 50 μM Ca^{2+} (Fig. 3C).
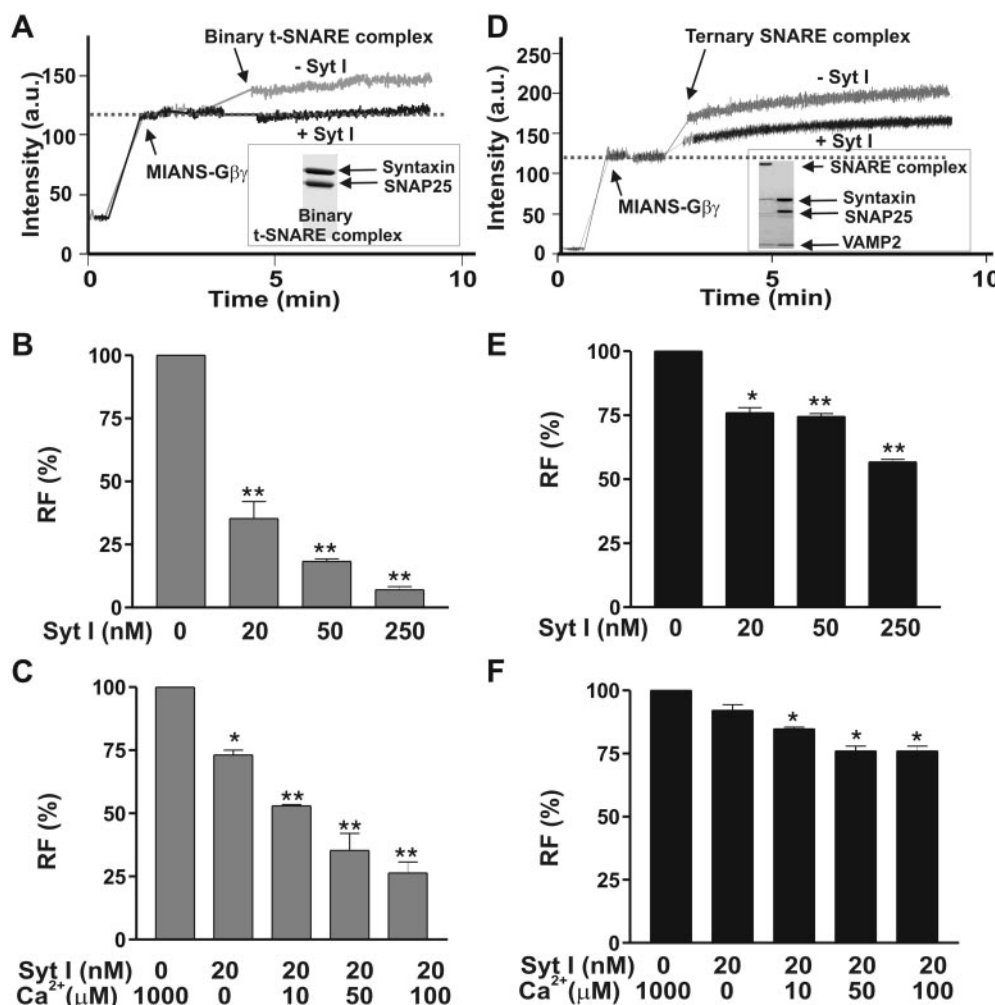

Fig. 3. Gβγ-mediated inhibition of the synaptotagmin/SNARE interaction is diminished at high Ca^{2+}-concentrations. A, preincubation with synaptotagmin (SytI) abrogates binding of Gβγ to the binary t-SNARE complex, indicating competition. Binary t-SNARE complexes were assembled with syntaxin1A and SNAP25 in a 1:1 ratio, as shown by SDS-PAGE/Coomassie staining analysis (inset). Binding of 1 μM binary t-SNARE to 20 nM MAINS-Gβγ with (+ synaptotagmin) or without (− synaptotagmin) 250 nM synaptotagmin was measured by fluorescence enhancement in 50 μM Ca^{2+}. B, competition for binary t-SNARE binding is dose-dependent. The Gβγ/t-SNARE interaction was monitored as described in A, and binding in the absence of synaptotagmin was normalized to 100%. Percentage of RF is plotted against synaptotagmin protein concentration in 50 μM Ca^{2+}. C, competition for binary t-SNARE binding is dependent on [Ca^{2+}]. Different concentration of Ca^{2+} (0–100 μM) as noted was applied, and percentage of RF was monitored. D, synaptotagmin and Gβγ compete for binding to the ternary SNARE complex. In vitro reassembled ternary SNARE complex showed an SDS- and heat-stable species (inset, lane 1) that dissociated by additional heat treatment (inset, lane 2). Binding of the ternary SNARE complex with MIANS-Gβγ with or without 250 nM synaptotagmin was performed as described for A. E, competition for ternary SNARE binding is dependent on the concentration of synaptotagmin. F, competition for ternary SNARE binding is dependent on [Ca^{2+}]. A and D depict typical results from at least three experiments. Data are represented as mean ± S.E.M. (n = 3).

Interactions of both Gβγ and synaptotagmin with the ternary SNARE complex modify the dilation of the vesicle fusion pore (Bai et al., 2004; Photowala et al., 2006). Thus, we tested the hypothesis that Gβγ competes with synaptotagmin for binding to the ternary SNARE complex. We first measured the Gβγ/SNARE interaction by determining the change in fluorescence of 20 nM MIANS-Gβγ upon addition of the ternary SNARE complex. Addition of 1 μM SNARE complex induced an increase of fluorescence intensity (Fig. 3D). This increase was reduced by inclusion of 250 nM synaptotagmin, indicating that Gβγ and synaptotagmin compete for binding to the ternary SNARE complex. In addition, competition by synaptotagmin and the resulting reduced fluorescence changes were dependent on the concentration of synaptotagmin (Fig. 3E) and the concentration of Ca^{2+} (Fig. 3F). Together, these data suggest that indeed Gβγ and synaptotagmin compete for binding to the ternary SNARE complex.

Gβγ and Synaptotagmin Competed for Binding to the Individual t-SNAREs (Syntaxin 1A and SNAP25) but Not the Vesicular SNARE (VAMP2). The H3 domain of syntaxin1A and the C terminus of SNAP25 provide interaction regions for Gβγ and synaptotagmin. We saw significantly more efficient competition between Gβγ and synaptotagmin in the context of binary t-SNAREs than ternary SNARE complexes. Therefore, we measured the individual contributions of SNARE components to competition between Gβγ and synaptotagmin.

First, to determine whether Gβγ and synaptotagmin compete for binding to syntaxin1A or SNAP25, the interaction of 20 nM MIANS-Gβγ with syntaxin1A and SNAP25 was monitored with or without preincubation of the SNARE proteins with 20 nM synaptotagmin. The interactions between Gβγ and SNARE proteins were unaffected by Ca^{2+} in the absence of synaptotagmin (data not shown). In the absence of Ca^{2+}, we observed a slight, statistically insignificant decrease in Gβγ binding to both syntaxin1A (Fig. 4A) and SNAP25 (Fig. 4B) upon preincubation of the SNARE proteins with 20 nM synaptotagmin. However, in 100 μM Ca^{2+}, the ability of synaptotagmin to compete for binding to SNAREs was

greatly enhanced. Syntaxin1A binding to Gβγ was reduced by 48% (Fig. 4A), and binding of SNAP25 to Gβγ was reduced by 78% (Fig. 4B). Thus, Gβγ competes with Ca^{2+}-synaptotagmin for binding to both syntaxin1A and SNAP25.

We observed a direct interaction between Gβγ and VAMP2 (Fig. 1, B and D). An earlier study suggested that synaptotagmin interacts with VAMP2 (Fukuda, 2002), leading to the possibility that this protein forms an additional site of competition between Gβγ and synaptotagmin. However, the existence of a direct synaptotagmin/VAMP2 interaction remains controversial (Chapman et al., 1995). Consequently, we monitored the Gβγ interaction with VAMP2 with or without preincubation of VAMP2 with synaptotagmin in the presence or absence of Ca^{2+}. No alteration in Gβγ binding to VAMP2 by synaptotagmin was observed, suggesting that Gβγ and synaptotagmin do not share a binding region on VAMP2 (Fig. 4C). This result may explain why competition at the ternary SNARE complex seems to favor Gβγ binding compared with competition at the binary t-SNARE: in the ternary SNARE complex, Gβγ binding is enhanced by an additional binding site within VAMP2 that is unaffected by synaptotagmin I. Thus, its ability to compete with Gβγ in the ternary SNARE complex is decreased.

The C Terminus of SNAP25 in the Ternary SNARE Complex Was Important for Gβγ-Synaptotagmin Competition. We have shown that BoNT/A, which specifically removes the C-terminal nine amino acids from SNAP25, greatly reduced the inhibitory effect of Gβγ on regulated exocytosis (Blackmer et al., 2001; Gerachshenko et al., 2005). We propose that this reduction can be explained if removal of these residues diminishes Gβγ competition with synaptotagmin for binding to the t-SNAREs and the ternary SNARE complex in vivo. Therefore, we examined the contribution of the C terminus of SNAP25 in the competition between Gβγ and synaptotagmin within the ternary SNARE complex. It is noteworthy that whereas BoNT/A cleavage of SNAP25 reduced binding of synaptotagmin and Gβγ individually, significant interactions were still observed (Fig. 2D). Thus, it was important to quantify the interactions using the fluores-
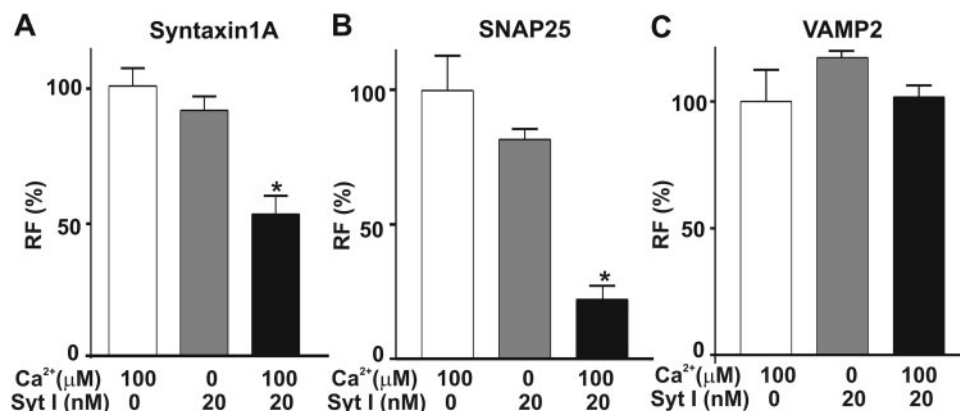

Fig. 4. Gβγ and synaptotagmin compete for binding to SNAP25 and syntaxin1A but not to VAMP2. A, Gβγ competes with synaptotagmin for binding to syntaxin1A. Competition assays were performed as described for Fig. 3. The relative change in fluorescence of 20 nM MIANS-Gβγ in 100 μM Ca^{2+} upon addition of 0.5 μM syntaxin1A was normalized to 100%. Addition of 20 nM synaptotagmin in the absence of Ca^{2+} induced a slight decrease in the Gβγ/syntaxin1A interaction, but inclusion of both 20 nM synaptotagmin and 100 μM Ca^{2+} reduced binding by approximately 50%. B, Gβγ competes with synaptotagmin for binding to SNAP25. Synaptotagmin (20 nM) caused a slight decrease in the interaction of 20 nM MIANS-Gβγ with 2 μM SNAP25 in the absence of Ca^{2+}, whereas inclusion of both 20 nM synaptotagmin and 100 μM Ca^{2+} reduced binding by approximately 80%. C, Gβγ and synaptotagmin do not compete for binding to VAMP2. The change in MIANS-Gβγ fluorescence upon addition of 2 μM VAMP2, normalized to 100%, was not reduced significantly in the presence of 20 nM synaptotagmin, with or without 100 μM Ca^{2+}. Data are presented as mean ± S.E.M. ($n = 3$).

cent binding assay to determine whether this cleavage shifted the G$\beta\gamma$/synaptotagmin competition toward synaptotagmin binding.

To test the relative contributions of the C terminus of SNAP25 in binding G$\beta\gamma$ and synaptotagmin, we quantified binding to ternary SNARE complexes comprising syntaxin1A, VAMP2, and SNAP25Δ9. Competition by synaptotagmin for G$\beta\gamma$ binding to SNARE complex that contains SNAP25Δ9 was increased compared with the wild-type SNARE complex at 50 μM Ca^{2+} (Fig. 5A). This finding is consistent with a model in which the nine C-terminal amino acids of SNAP25 represent an important determinant mediating exclusion of synaptotagmin binding by G$\beta\gamma$.

We then determined the concentration dependence of the synaptotagmin competition. The strength of synaptotagmin competition in SNARE complexes formed with SNAP25Δ9 increased dramatically compared with the wild type SNARE complex (Fig. 5B). These results suggest that the C-terminal nine amino acids of SNAP25 are more critical for G$\beta\gamma$ than for synaptotagmin binding. These data support the dramatic loss of inhibitory effect of G$\beta\gamma$ in the BoNT/A-treated synapse (Gerachshenko et al., 2005).

The 5-HT Mediated Regulation of Exocytosis Was Diminished with High [Ca^{2+}] at the Lamprey Giant Synapse. What role does G$\beta\gamma$-synaptotagmin I competition for SNARE complexes play at synapses? At lamprey giant synapses, we have shown that 5-HT inhibits transmitter release through direct G$\beta\gamma$/SNARE complex interactions. 5-HT mediated G$\beta\gamma$ does not inhibit voltage-gated Ca^{2+} channels in this preparation but acts directly on the ternary SNARE complex to inhibit exocytosis (Blackmer et al., 2001;

Takahashi et al., 2001; Gerachshenko et al., 2005). From our in vitro study, we hypothesized that G$\beta\gamma$-mediated inhibition requires competition between G$\beta\gamma$ and Ca^{2+}-dependent synaptotagmin binding on the SNARE complex. These findings suggested that the effect of GPCR-mediated activation of
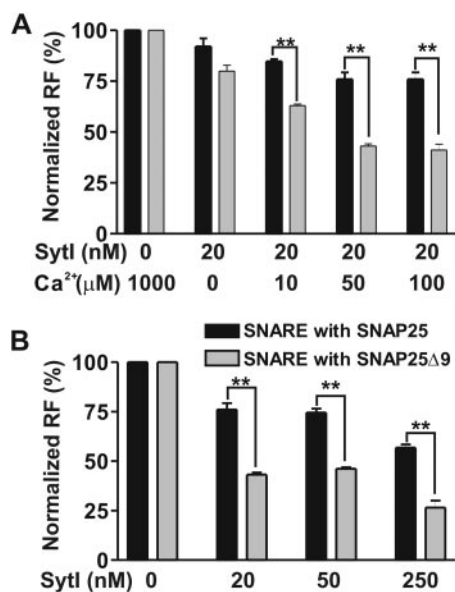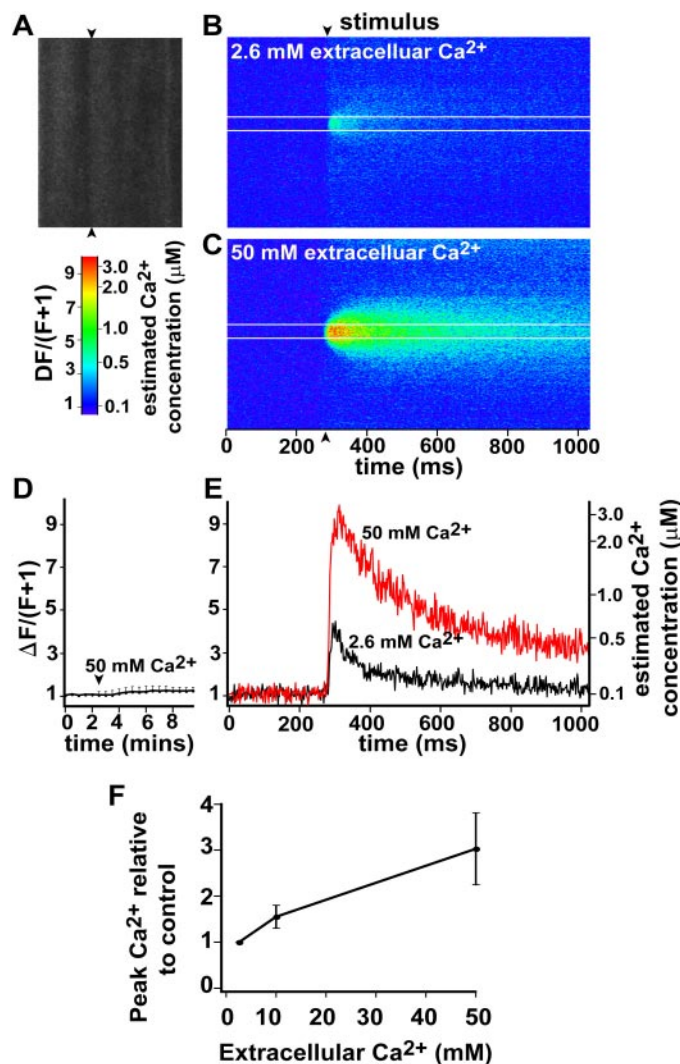

Fig. 6. Raising extracellular [Ca^{2+}] increases intracellular [Ca^{2+}] transients in a presynaptic terminal. A, lamprey giant axons labeled retrogradely with a Ca^{2+}-sensitive dye (Fluo-4 dextran high affinity) and imaged with confocal microscopy. To quantify rapid action potential-induced Ca^{2+} transients, high-speed line scanning of Ca^{2+} entry (500 Hz) was repeated at the edge of the axon marked with the arrowheads. B–F, raising extracellular [Ca^{2+}] enhances action-potential-induced Ca^{2+} influx. B, a single action potential in the axon evoked at the time point marked by the arrowhead caused a localized Ca^{2+} transient in the axon. The line scan is pseudocolored with the lookup table shown below A. The pixel values were measured and, after background substration, images were normalized to the baseline level of fluorescence [$\Delta F/(F + 1)$]. C, increasing the extracellular Ca^{2+} concentration from 2.6 to 50 mM markedly enhanced the amplitude of the Ca^{2+} transient. D, during wash-in of 50 mM Ca^{2+} the resting fluorescence was monitored at 30-s intervals. A small increase in the resting fluorescence was observed. Fluorescence is recorded to the same scale as E. E, the Ca^{2+} transients were measured between the white horizontal lines in B and C to quantify Ca^{2+} entry. Estimates of recorded Ca^{2+} transient amplitudes were made as described under *Materials and Methods*. The calculated Ca^{2+} concentration scale for this estimate is shown to the right. F, the relative effect of raising extracellular Ca^{2+} concentration on the amplitude of the axonal Ca^{2+} transient is recorded. Note that high extracellular Ca^{2+} concentrations have a proportionately smaller effect on the amplitudes of the recorded intracellular transient.

Fig. 5. The C-terminal nine amino acids of SNAP25 comprise a critical region for competition between G$\beta\gamma$ and synaptotagmin. G$\beta\gamma$ competition with synaptotagmin to bind ternary SNARE complex was made up of SNAP25 (black bar) or SNAP25Δ9 (gray bar). G$\beta\gamma$ and SNARE complex binding was normalized to 100% fluorescence in the presence of 1 mM Ca^{2+} and in the absence of synaptotagmin. Competition by synaptotagmin for G$\beta\gamma$ binding to SNARE containing SNAP25Δ9 was increased compared with the wild-type SNARE complex. A, competition for binding to SNARE (SNAP25Δ9) is more sensitive to [Ca^{2+}]. B, synaptotagmin I competes in a dose-dependent manner with G$\beta\gamma$ for binding to SNARE, more potently with SNAP25Δ9. Data are represented as mean $\pm$ S.E.M. ($n = 3$).

Gβγ would be mitigated by raising the synaptic terminal Ca^{2+} concentration.

We tested this possibility using paired recordings between giant axons and postsynaptic neurons in lamprey synapse. To increase action potential-evoked intracellular Ca^{2+} concentrations, we raised extracellular Ca^{2+} concentrations (Fig. 6, A–C). We first quantified the consequent effect on evoked presynaptic Ca^{2+} entry. Axons were filled with a Ca^{2+} sensitive dye (Fluo-4 dextran high affinity) and imaged with confocal microscopy. Action potential-evoked presynaptic fluorescence transients were imaged under increasing extracellular Ca^{2+} (2.6, 10, and 50 mM; Fig. 6, B and C, and data not shown). The relationship between extracellular Ca^{2+} concentrations and the fluorescence transient was alinear (Fig. 6E). Therefore, to calculate the relationship between extracellular Ca^{2+} and the intracellular Ca^{2+} transient amplitude, we determined the peak intracellular Ca^{2+} during the transients. The affinity of the dye (1.2 μM) was obtained from fluorescence curves that showed a 120-fold increase in fluorescence between 0 μM Ca^{2+} and saturation (41 μM) at a physiological temperature. Using these data and the resting $[Ca^{2+}]$ in lamprey axons (approximately 100 nM), we estimated the peak transient intracellular Ca^{2+} (Fig. 6E). Extracellular Ca^{2+} (50 mM) slightly increased basal presynaptic intracellular Ca^{2+} (Fig. 6D). However, the evoked fluorescence transient, and therefore its peak Ca^{2+} concentration, was markedly increased (Fig. 6E). Note that absolute Ca^{2+} concentrations calculated in this way underestimate the concentration at the vesicle fusion site because we cannot image with sufficient resolution to resolve the close spatial relationship between Ca^{2+} channels and the release machinery (Adler et al., 1991). Consequently, we used these data to calculate the relative amplitude of the Ca^{2+} transient at extracellular concentrations of 10 and 50 mM (Fig. 6F) normalized to control (2.6 mM).

We then tested the effect of increased Ca^{2+} on 5-HT-mediated presynaptic inhibition. At a control extracellular Ca^{2+} concentration (2.6 mM), 5-HT (600 nM) reduced the EPSC to $55.9 \pm 7.3\%$ of control ($n = 5$; $P < 0.05$). The EPSC fully recovered upon 5-HT removal (Fig. 7A, top). Extracellular Ca^{2+} (50 mM) increased the EPSC amplitude to $129.7 \pm 4.7\%$ of control ($n = 5$; $P < 0.01$), but 600 nM 5-HT caused no inhibition (Fig. 7A, bottom; EPSC was $97.1 \pm 8.1\%$ of the EPSC modified by 50 mM Ca^{2+}; $n = 5$ pairs). At 50 mM extracellular Ca^{2+}, even a saturating dose of 5-HT (10 μM) resulted in only a slight reduction in the EPSC [response was $71.3 \pm 0.9\%$ of the control response modified by high Ca^{2+} ($n = 3$, $P > 0.05$), compared with a reduction to 20% of control in normal Ca^{2+} (Takahashi et al., 2001)] (Fig. 7, B and C). We also confirmed that 5-HT does not change Ca^{2+} influx in lamprey synapses (Blackmer et al., 2001; Takahashi et al., 2001) treated with 50 mM extracellular Ca^{2+} concentration (Supplementary Figure S2). Thus, increased intracellular Ca^{2+} transients attenuated GPCR mediated presynaptic inhibition.

High Extracellular Ca^{2+} Attenuated the Presynaptic Inhibitory Effect of Gβγ. We have shown that the reduction of the EPSC upon activation of 5-HT receptors is caused by liberated Gβγ (Blackmer et al., 2001; Gerachshenko et al., 2005). Here, we examined the effects of manipulating intracellular Ca^{2+} on EPSC inhibition by free Gβγ introduced through direct injection of purified Gβγ protein into presynaptic axons. We compared Gβγ-mediated inhibition of exocytosis at a control (2.6 mM) and a raised Ca^{2+} concentration (10 mM); the latter increased the EPSC amplitude (Fig. 8A) to $122 \pm 2\%$ of control ($n = 3$). In four more paired recordings, we probed the effect of raising Ca^{2+} concentrations on inhibition by presynaptic Gβγ. In control Ca^{2+} (2.6 mM), Gβγ injection significantly reduced the EPSC, as described previously (Blackmer et al., 2001), to $37 \pm 12\%$ (Fig. 8, B and C). In the same pairs, the Ca^{2+} concentration was raised to 10 mM and Gβγ inhibition was reversed (10 mM; Fig. 8, B and C; EPSC was $100 \pm 9\%$ of control). Thus raised Ca^{2+} transient amplitudes significantly attenuated the inhibitory effect of presynaptic Gβγ. The effects of both 5-HT and presynaptic Gβγ injection are attenuated by enhancing the amplitude of the action potential evoked presynaptic Ca^{2+} transient.
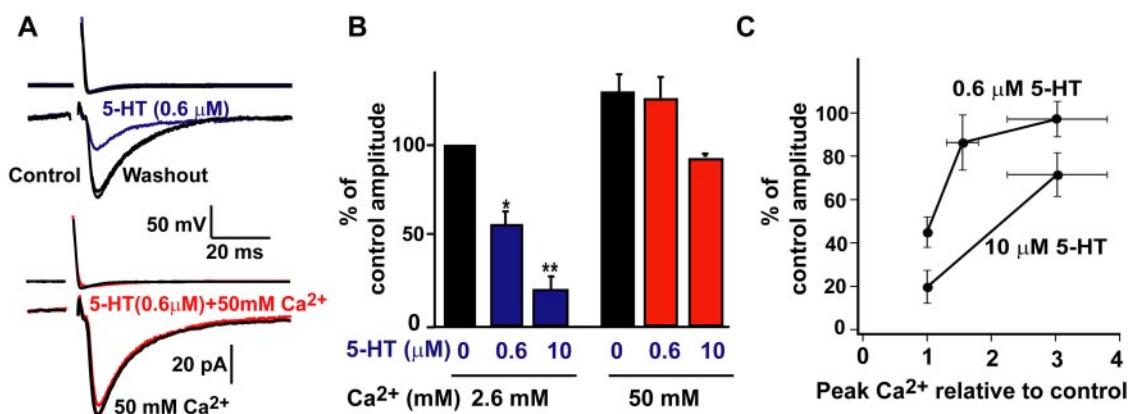

Fig. 7. Raising extracellular $[Ca^{2+}]$ decreases 5-HT-mediated inhibition of exocytosis in a presynaptic terminal. A, increasing extracellular $[Ca^{2+}]$ and, therefore, the intracellular $[Ca^{2+}]$ transients abrogates 5-HT-mediated inhibition of exocytosis. In a paired recording of presynaptic action potentials (upward peaks) and EPSCs (downward current peaks), a moderate dose of 5-HT (0.6 μM) applied in normal extracellular $[Ca^{2+}]$ (2.6 mM) caused inhibition of exocytosis (blue). The EPSC recovered after 5-HT washout (top). The effect of 0.6 μM 5-HT is completely abrogated in 50 mM extracellular $[Ca^{2+}]$ (red, bottom). B, pooled data show the 5-HT-mediated inhibition in 2.6 and 50 mM Ca^{2+} ($n = 4$–5, ∗∗, $P < 0.01$; ∗, $P < 0.05$). In control extracellular Ca^{2+} concentration, 0.6 and 10 μM 5-HT significantly reduced the amplitude (blue). In 50 mM extracellular Ca^{2+}, 0.6 μM 5-HT no longer inhibited synaptic release, and a saturating dose of 10 μM 5-HT slightly decreased the amplitude but was not statistically significant (red). C, a comparison of the ability of moderate (0.6 μM) or high (10 μM) doses of 5-HT to inhibit exocytosis reveals that the level of exocytotic inhibition is highly dependent on the levels of both G protein activation and intracellular Ca^{2+}. The relative level of intracellular Ca^{2+} is indicated on the x-axis, whereas the degree of inhibition of exocytosis was measured as the EPSC response relative to control (no 5-HT) (y-axis).

Discussion

In primed vesicles, Ca^{2+} effects exocytosis in part by increasing synaptotagmin's affinity for the primed SNARE complex (Perin et al., 1990; Schiavo et al., 1997; Yoshihara and Littleton, 2002; Bai et al., 2004; Wang et al., 2006). $G\beta\gamma$ liberated by inhibitory $G_{i/o}$-coupled GPCRs inhibits neurotransmitter release by at least two mechanisms: inhibition of presynaptic Ca^{2+} entry at many synapses by modulating voltage-gated calcium channels (Herlitze et al., 1996; Ikeda, 1996), as well as interaction with the ternary SNARE complex late in membrane fusion (Blackmer et al., 2005; Gerachshenko et al., 2005). Here we show that $G\beta\gamma$ interacts with SNARE proteins and that this binding is not directly modified by calcium. $G\beta\gamma$ interacts with VAMP2 at a site different from synaptotagmin's in-

Fig. 8. High extracellular Ca^{2+} blocks the presynaptic inhibitory effect of $G\beta\gamma$. A, increased extracellular $[Ca^{2+}]$ causes a slight increase in exocytosis. A paired cell recording (top, presynaptic action potentials; bottom, resultant EPSCs) demonstrates the effect of raising extracellular Ca^{2+} from 2.6 (black trace) to 10 mM (gray). B, the effect of presynaptic $G\beta\gamma$ injection is reversed by raising the extracellular Ca^{2+} concentration. The responses observed in A were inhibited by injection of $G\beta\gamma$ (blue). Subsequently raising the extracellular Ca^{2+} concentration reversed this inhibition (red). C, pooled data showing the effect of raising extracellular $[Ca^{2+}]$ on the control synaptic responses and on the response in 10 mM Ca^{2+}. Extracellular Ca^{2+} (10 mM) enhanced the control response to $122 \pm 2\%$ of control ($n = 3$) (gray bar). In a further 4 paired cell recordings, presynaptic injection of $G\beta\gamma$ inhibited control responses to $37 \pm 12\%$ of control (blue). Raising the extracellular Ca^{2+} concentration to 10 mM caused a recovery to $100 \pm 9\%$ of control (red).

teraction. Perhaps the $G\beta\gamma$/VAMP2 interaction strengthens $G\beta\gamma$ binding to the SNARE complex, whereas occlusion of synaptotagmin I binding occurs through the t-SNARE components (syntaxin1A and SNAP25) in the ternary SNARE complex. In addition, $G\beta\gamma$ binds directly to the t-SNAREs SNAP25 and syntaxin1A at sites similar to those used by synaptotagmin to interact with these proteins in a Ca^{2+}-dependent manner. This sets up a potent competition with the Ca^{2+} sensor to inhibit regulated exocytosis. This differential Ca^{2+} requirement can lead to a Ca^{2+}-sensitivity of the $G\beta\gamma$ inhibition of SNARE/synaptotagmin complex formation: at low and moderate Ca^{2+} concentrations, the presence of inhibitory signals generates $G\beta\gamma$ that competes with synaptotagmin for binding to SNARE, leading to inhibition of exocytosis. At high Ca^{2+} concentrations, the affinity of synaptotagmin for SNARE increases, whereas the $G\beta\gamma$/SNARE affinity remains steady, and thus high synaptic activity overrides the inhibition by $G\beta\gamma$.

At the synapse, after C-terminal truncation of SNAP-25 with BoNT/A, exocytosis recovers in high Ca^{2+} in many preparations, including the lamprey (Gerachshenko et al., 2005), presumably because high Ca^{2+} enhances the residual synaptotagmin/SNARE interaction that remains after BoNT/A treatment. However, the affinity of $G\beta\gamma$ for the modified SNARE complex is much lower, and $G\beta\gamma$ therefore competes less well with synaptotagmin for the same site, particularly at raised intracellular Ca^{2+}. These findings led to a testable hypothesis: at the synapse, larger evoked Ca^{2+} transients should prevent $G\beta\gamma$-mediated presynaptic inhibition induced by 5-HT. Accordingly, in the lamprey giant synapse, although 5-HT powerfully inhibits exocytosis through $G\beta\gamma$ interaction with the SNARE complex (Silinsky, 1984; Man-Son-Hing et al., 1989; Blackmer et al., 2001, 2005; Takahashi et al., 2001; Chen et al., 2005; Gerachshenko et al., 2005), we observed that enhancing the Ca^{2+} transient reversed this inhibition (Figs. 6 and 7). These data are consistent with the biochemical results showing that inhibition of synaptotagmin/SNARE complex interaction by $G\beta\gamma$ is sensitive to Ca^{2+}. Although Ca^{2+} could have other effects in the synapse, the fact that synaptotagmin is thought to be the major Ca^{2+} receptor for exocytosis (Bai et al., 2004; Maximov and Sudhof, 2005; Wang et al., 2006) suggests that $G\beta\gamma$ may work physiologically by competing with Ca^{2+}-synaptotagmin for SNARE, leading to inhibition of exocytosis. $G\beta\gamma$ also has many other targets, and enhancing intracellular Ca^{2+} could modify the effects of these interactions on exocytosis. The most obvious other $G\beta\gamma$ effector is the voltage-gated Ca^{2+} channel, which has been shown by many investigators to be inhibited by $G\beta\gamma$. However, $G\beta\gamma$ has no effect on Ca^{2+} entry even at 50 mM extracellular Ca^{2+}, because 5-HT does not modify evoked Ca^{2+} entry (Supplementary Figure S2).

This Ca^{2+}-dependent regulation may complete a physiological feedback loop, because $G\beta\gamma$ may control both Ca^{2+} influx through voltage-gated Ca^{2+} channels (Herlitze et al., 1996; Ikeda, 1996) and access of the Ca^{2+} effector synaptotagmin to its site on the SNARE. Our data suggest that this competition is elegantly controlled by overlap of the binding sites of $G\beta\gamma$ and synaptotagmin at the SNARE proteins SNAP25 and syntaxin. In a further level of regulation, during repetitive stimulation, buildup of intracellular Ca^{2+} concentration may reverse $G\beta\gamma$ inhibition. Thus, depending on presynaptic $G_{i/o}$-coupled GPCR activation and Ca^{2+} influx in
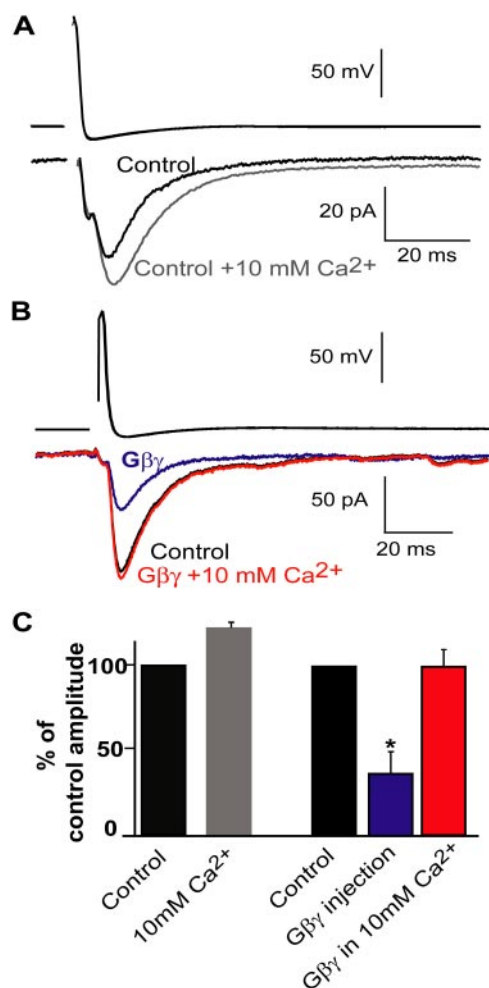
response to synaptic activity, a range of efficiencies of exocytosis potentially exists. Thus, we predict that a complex and dynamic regulation of vesicle fusion properties will occur. Finally, at low levels of inhibitory GPCR signaling, G$\beta\gamma$ causes kiss-and-run exocytosis in lamprey synapses (Photowala et al., 2006) and adrenal chromaffin cells (data not shown) (Chen et al., 2005). In hippocampal neurons, sustained stimulus trains forcing high presynaptic Ca^{2+} concentrations change fusion from a state dominated by kiss-and-run to one favoring full fusion (Harata et al., 2006). However, the exact Ca^{2+} concentrations required to reverse G$\beta\gamma$-mediated presynaptic inhibition are likely to exceed those obtained by residual Ca^{2+} during short bursts of stimuli, in which saturating doses of 5-HT remains effective (Takahashi et al., 2001). Thus, we speculate that the dynamic relationship between inhibitory GPCRs and presynaptic Ca^{2+} constantly modifies the nature of the vesicle fusion event itself.

References

Adler EM, Augustine GJ, Duffy SN, and Charlton MP (1991) Alien intracellular calcium chelators attenuate neurotransmitter release at the squid giant synapse. *J Neurosci* **11:**1496–1507.

Bai J, Wang CT, Richards DA, Jackson MB, and Chapman ER (2004) Fusion pore dynamics are regulated by synaptotagmin*t-SNARE interactions. *Neuron* **41:**929–942.

Bennett MK, Calakos N, and Scheller RH (1992) Syntaxin: a synaptic protein implicated in docking of synaptic vesicles at presynaptic active zones. *Science* **257:**255–259.

Blackmer T, Larsen EC, Bartleson C, Kowalchyk JA, Yoon EJ, Preininger AM, Alford S, Hamm HE, and Martin TF (2005) G protein betagamma directly regulates SNARE protein fusion machinery for secretory granule exocytosis. *Nat Neurosci* **8:**421–425.

Blackmer T, Larsen EC, Takahashi M, Martin TF, Alford S, and Hamm HE (2001) G protein betagamma subunit-mediated presynaptic inhibition: regulation of exocytotic fusion downstream of Ca^{2+} entry. *Science* **292:**293–297.

Blanton MG, Lo Turco JJ, and Kriegstein AR (1989) Whole cell recording from neurons in slices of reptilian and mammalian cerebral cortex. *J Neurosci Methods* **30:**203–210.

Chapman ER, Hanson PI, An S, and Jahn R (1995) Ca^{2+} regulates the interaction between synaptotagmin and syntaxin 1. *J Biol Chem* **270:**23667–23671.

Chen XK, Wang LC, Zhou Y, Cai Q, Prakriya M, Duan KL, Sheng ZH, Lingle C, and Zhou Z (2005) Activation of GPCRs modulates quantal size in chromaffin cells through G(betagamma) and PKC. *Nat Neurosci* **8:**1160–1168.

Chen YA, Scales SJ, Jagath JR, and Scheller RH (2001) A discontinuous SNAP-25 C-terminal coil supports exocytosis. *J Biol Chem* **276:**28503–28508.

Chen YA, Scales SJ, Patel SM, Doung YC, and Scheller RH (1999) SNARE complex formation is triggered by Ca^{2+} and drives membrane fusion. *Cell* **97:**165–174.

Elhamdani A, Azizi F, and Artalejo CR (2006) Double patch clamp reveals that transient fusion (kiss-and-run) is a major mechanism of secretion in calf adrenal chromaffin cells: high calcium shifts the mechanism from kiss-and-run to complete fusion. *J Neurosci* **26:**3030–3036.

Elhamdani A, Palfrey HC, and Artalejo CR (2001) Quantal size is dependent on stimulation frequency and calcium entry in calf chromaffin cells. *Neuron* **31:**819–830.

Ferrer-Montiel AV, Gutierrez LM, Apland JP, Canaves JM, Gil A, Viniegra S, Biser JA, Adler M, and Montal M (1998) The 26-mer peptide released from SNAP-25 cleavage by botulinum neurotoxin E inhibits vesicle docking. *FEBS Lett* **435:**84–88.

Fukuda M (2002) Vesicle-associated membrane protein-2/synaptobrevin binding to synaptotagmin I promotes O-glycosylation of synaptotagmin I. *J Biol Chem* **277:**30351–30358.

Gerachshenko T, Blackmer T, Yoon EJ, Bartleson C, Hamm HE, and Alford S (2005)

Gbetagamma acts at the C terminus of SNAP-25 to mediate presynaptic inhibition. *Nat Neurosci* **8:**597–605.

Gerona RR, Larsen EC, Kowalchyk JA, and Martin TF (2000) The C terminus of SNAP25 is essential for Ca^{2+}-dependent binding of synaptotagmin to SNARE complexes. *J Biol Chem* **275:**6328–6336.

Han X and Jackson MB (2006) Structural transitions in the synaptic SNARE complex during Ca^{2+}-triggered exocytosis. *J Cell Biol* **172:**281–293.

Harata NC, Choi S, Pyle JL, Aravanis AM, and Tsien RW (2006) Frequency-dependent kinetics and prevalence of kiss-and-run and reuse at hippocampal synapses studied with novel quenching methods. *Neuron* **49:**243–256.

Herlitze S, Garcia DE, Mackie K, Hille B, Scheuer T, and Catterall WA. Modulation of Ca^{2+} channels by G-protein beta gamma subunits. *Nature* 380:258–262, 1996.

Ikeda SR (1996) Voltage-dependent modulation of N-type calcium channels by G-protein beta gamma subunits. *Nature* **380:**255–258.

Jarvis SE, Barr W, Feng ZP, Hamid J, and Zamponi GW (2002) Molecular determinants of syntaxin 1 modulation of N-type calcium channels. *J Biol Chem* **277:** 44399–44407.

Man-Son-Hing H, Zoran MJ, Lukowiak K, and Haydon PG (1989). A neuromodulator of synaptic transmission acts on the secretory apparatus as well as on ion channels. *Nature* **341:**237–239.

Margittai M, Otto H, and Jahn R (1999) A stable interaction between syntaxin 1a and synaptobrevin 2 mediated by their transmembrane domains. *FEBS Lett* **446:**40–44.

Maximov A and Sudhof TC (2005) Autonomous function of synaptotagmin 1 in triggering synchronous release independent of asynchronous release. *Neuron* **48:** 547–554.

Mazzoni MR, Malinski JA, and Hamm HE (1991) Structural analysis of rod GTP-binding protein, Gt. Limited proteolytic digestion pattern of Gt with four proteases defines monoclonal antibody epitope. *J Biol Chem* **266:**14072–14081.

Morimoto T, Popov S, Buckley KM, and Poo MM (1995) Calcium-dependent transmitter secretion from fibroblasts: modulation by synaptotagmin I. *Neuron* **15:**689–696.

Perin MS, Fried VA, Mignery GA, Jahn R, and Sudhof TC (1990) Phospholipid binding by a synaptic vesicle protein homologous to the regulatory region of protein kinase C. *Nature* **345:**260–263.

Phillips WJ and Cerione RA (1991) Labeling of the beta gamma subunit complex of transducin with an environmentally sensitive cysteine reagent. Use of fluorescence spectroscopy to monitor transducin subunit interactions. *J Biol Chem* **266:** 11017–11024.

Photowala H, Blackmer T, Schwartz E, Hamm HE, and Alford S (2006) G protein beta{gamma}-subunits activated by serotonin mediate presynaptic inhibition by regulating vesicle fusion properties. *Proc Natl Acad Sci U S A* **103:**4281–4286.

Rizo J, Chen X, and Arac D (2006) Unraveling the mechanisms of synaptotagmin and SNARE function in neurotransmitter release. *Trends Cell Biol*.

Schiavo G, Stenbeck G, Rothman JE, and Sollner TH (1997) Binding of the synaptic vesicle v-SNARE, synaptotagmin, to the plasma membrane t-SNARE, SNAP-25, can explain docked vesicles at neurotoxin-treated synapses. *Proc Natl Acad Sci U S A* **94:**997–1001.

Searl TJ and Silinsky EM (2005) Modulation of Ca^{2+}-dependent and Ca^{2+}-independent miniature endplate potentials by phorbol ester and adenosine in frog. *Br J Pharmacol* **145:**954–962.

Silinsky EM (1984) On the mechanism by which adenosine receptor activation inhibits the release of acetylcholine from motor nerve endings. *J Physiol* **346:**243–256.

Sollner T, Bennett MK, Whiteheart SW, Scheller RH, and Rothman JE (1993) A protein assembly disassembly pathway in vitro that may correspond to sequential steps of synaptic vesicle docking, activation, and fusion. *Cell* **75:**409–418.

Sorensen JB, Wiederhold K, Muller EM, Milosevic I, Nagy G, de Groot BL, Grubmuller H, and Fasshauer D (2006) Sequential N- to C-terminal SNARE complex assembly drives priming and fusion of secretory vesicles. *EMBO J* **25:**955–966.

Takahashi M, Freed R, Blackmer T, and Alford S (2001) Calcium influx-independent depression of transmitter release by 5-HT at lamprey spinal cord synapses. *J Physiol* **532:**323–336.

Wang CT, Bai J, Chang PY, Chapman ER, and Jackson MB (2006) Synaptotagmin-Ca^{2+} triggers two sequential steps in regulated exocytosis in rat PC-12 cells: fusion pore opening and fusion pore dilation. *J Physiol* **570:**295–307.

Wang CT, Grishanin R, Earles CA, Chang PY, Martin TF, Chapman ER, and Jackson MB (2001) Synaptotagmin modulation of fusion pore kinetics in regulated exocytosis of dense-core vesicles. *Science* **294:**1111–1115.

Wickelgren WO (1977) Physiological and anatomical characteristics of reticulospinalneurones in lamprey. *J Physiol* **270:**89–114.

Yoshihara M and Littleton JT (2002) Synaptotagmin I functions as a calcium sensor to synchronize neurotransmitter release. *Neuron* **36:**897–908.

Address correspondence to: Heidi E. Hamm, Department of Pharmacology, Vanderbilt University Medical School, 23rd Ave. South at Pierce, Nashville, TN 37232. E-mail: heidi.hamm@vanderbilt.edu